Available online at www.sciencedirect.com
SCIENCE DIRECT®

Journal of the European Ceramic Society 23 (2003) 2183–2191
www.elsevier.com/locate/jeurceramsoc

High temperature plastic deformation of 24–32 mol% yttria cubic stabilized zirconia (YCSZ) single crystals

Angela Gallardo-López, Diego Gómez-García, Julián Martínez-Fernández, Arturo Domínguez-Rodríguez*

Departamento de Física de la Materia Condensada, Universidad de Sevilla, Apdo 1065, 41080 Seville, Spain

Received 26 July 2002; received in revised form 9 January 2003; accepted 17 January 2003

Abstract

The high temperature mechanical properties of yttria fully-stabilised cubic zirconia (YCSZ) single crystals with yttria content of 24, 28 and 32 mol% have been studied. Creep experiments have been carried out in air and argon atmosphere at temperatures between 1400 and 1700 °C, under nominal stresses from 67 to 280 MPa. The samples were oriented for easy glide, that is, with the compression axis on the $<112>$ crystallographic direction, and lateral faces corresponding to {110} and {111} crystallographic planes. Using the phenomenological creep equation, the stress exponent, n, and activation energy, Q, have been estimated in two temperature ranges: 1400–1500 °C with $n \approx 6.8$ and $Q \approx 9.2$ eV, and 1500–1700 °C with $n \approx 4.7$ and $Q \approx 5.9$ eV. The strain rates obtained confirm that there is a very smooth increase in creep resistance with the yttria content for the studied range of composition. The dislocation substructure of the deformed samples has also been investigated via TEM. Conventional **g**·**b** analysis has been carried out and all the results have been compared to previous ones for lower yttria content YCSZ. On the basis of the creep parameters obtained and the microstructural observations, two deformation mechanisms are proposed, depending on the temperature used in the deformation experiments: glide controlled solute drag for the lower temperature range ($T \approx 1400$ °C) and climb controlled recovery creep for higher temperatures ($T \geqslant 1500$ °C).

Keywords: Creep; Electron microscopy; Single crystals; Y_2O_3–ZrO_2; ZrO_2

1. Introduction

Since the discovery of the increase of toughness by the martensitic transformation[1] in zirconium oxide (zirconia), the microstructure and mechanical properties of zirconia based ceramics have been thoroughly studied. The system ZrO_2–Y_2O_3 is probably the most suitable for high temperature applications, due to its good structural properties. It exhibits superplasticity for fine-grained polycrystals[2,3] and strong hardening either by solid solution[4,5] or precipitation.[6] For that purpose it is essential to study and understand its basic properties. Much work has been done to determine the influence of the yttria content in the mechanical properties of the system ZrO_2–Y_2O_3. However, one of the problems that still remains unsolved is the high-temperature mechanical behaviour ($T > 1400$ °C) of cubic crystals of completely yttria fully stabilised cubic zirconia (YCSZ) when the stabiliser (yttria) content is high >21 mol%.

The creep behaviour at high temperatures of YCSZ for yttria concentrations up to 21 mol% has been systematically studied,[7–9,12–14] and detailed microstructural analysis have been performed on the deformed samples.[12–17] The stress exponent and activation energy obtained for the most thoroughly studied compositions in the literature (9.4, 15, 18 and 21 mol%), as well as the dislocations substructure observed have been attributed to two deformation mechanisms which control strain-rate at different temperatures. In fact, both are operative in the whole temperature range, but with different kinetics. The transition temperature in the rate-controlling mechanism has been found between 1450 °C,[7] 1500 °C[9] and 1525 °C.[12] In the lower temperature range (1400–1500 °C), a solute drag mechanism has been proposed, while for higher temperatures, recovery creep has been reported. Other authors, however, propose a unique mechanism: recovery creep for $T \geqslant 1400$ °C.[18–23]

* Corresponding author.
E-mail address: adorod@us.es (A. Domínguez-Rodríguez).

0955-2219/03/$ - see front matter © 2003 Elsevier Ltd. All rights reserved.
doi:10.1016/S0955-2219(03)00047-5

In the range of yttria concentrations between 9.4 and 21 mol%,[4,5,7–17] a progressive hardening has been reported when increasing the amount of yttria. However, for yttria concentrations >21 mol% only isolated data of yield stress have been given in the literature.[24] The data plotted in Fig. 1, from constant strain-rate experiments, point out an apparent softening (decrease in the yield stress for yttria concentrations above 21 mol%).[24,25] At room temperature, however, recent works[26] report only small variations of microhardness for YCSZ with yttria content over 21 mol% (see Fig. 2). The preliminary results existing for high temperature[24] seemed to be an apparent contradiction with the expected hardening of YCSZ with higher yttria content reported in the range 9.4–21 mol%, so a study of the microscopical mechanisms controlling plastic deformation in this range of compositions 24–32 mol% appears rather interesting.

This study, carried out on YCSZ samples richer in yttria (24–32 mol%), is the logical extension of the previous ones (9.4[7] and 15–21 mol%[12,13]), so that the effect of yttria content on the high-temperature mechanical properties of YCSZ can be systematically evaluated and understood. For that reason, the experimental part has been carried out following a similar scheme as previous works,[7,12,13] and the macroscopic results from the mechanical tests have been correlated to TEM observations of the dislocation substructure to determine the mechanisms controlling deformation. Samples with 21 mol% yttria were also tested in creep to validate the results obtained for other compositions and the experimental procedure.

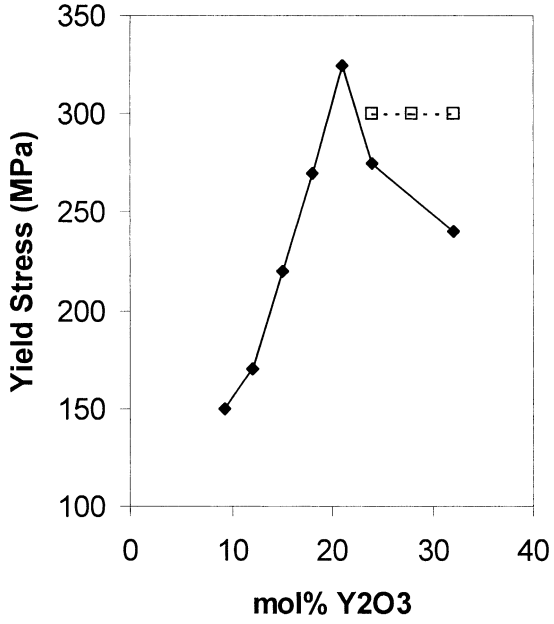

Fig. 1. Yield stress of YCSZ at 1400 °C and strain rate $\sim 5{\cdot}10^{-5}$ s^{-1} versus yttria content. Data from —◆— McClellan et al.[24] and ···□··· Gallardo-López et al.[25]

2. Experimental method

The YCSZ single crystals grown by skull-melting with 21, 24, 28 and 32 mol% were provided by Ceres Corporation (Massachusets, E.E.U.U.). The crystals were oriented by the Laue backscattered beam technique, using a Phillips X-ray generator, model PW 1720. Parallelepipeds with 2.5×2.5×5 mm were cut with a diamond saw. The compression axis of the samples (height of the parallelepiped) was the $\lfloor 1\bar{1}2 \rfloor$ direction, while the side faces corresponded to $\left(\bar{1}11\right)$ and (110) planes. The orientation of the samples was chosen in this way to activate the primary $(001)\lfloor 1\bar{1}0 \rfloor$ or "easy glide" slip system, with a Schmid factor of 0.47.[9,27]

Samples were polished with diamond paste to a 3 μm finish in order to minimise surface defects that could transform into cracks during creep. The temperatures used for the mechanical tests ranged from 1400 to 1700 °C, and the nominal stresses from 67 to 280 MPa. Measured strain rates $\dot{\varepsilon}$ varied between $\sim 10^{-8}$ and $\sim 10^{-5}$ s^{-1}. The deformation equipment used for experiments in argon was a prototype machine described elsewhere,[28] with silicon carbide rams and tungsten resistors for the furnace. The inert argon atmosphere was necessary to prevent oxidation of the furnace components. Tests in air were carried out in a universal Instron machine, model 1185, with special sapphire rams oriented along their c axes to prevent indentation of the pushing rods.

The strain of the sample was continually recorded versus time during creep, at a given load and temperature. From these data, the strain rate can be plotted versus strain ($\dot{\varepsilon}$ versus ε). Fig. 3 shows a typical creep curve of a 32 mol% YCSZ sample tested between 1450 and 1550 °C in Ar.

Data corresponding to the strain rate ($\dot{\varepsilon}$), stress (σ) and absolute temperature (T), were introduced into the high-temperature plastic deformation equation:[9]

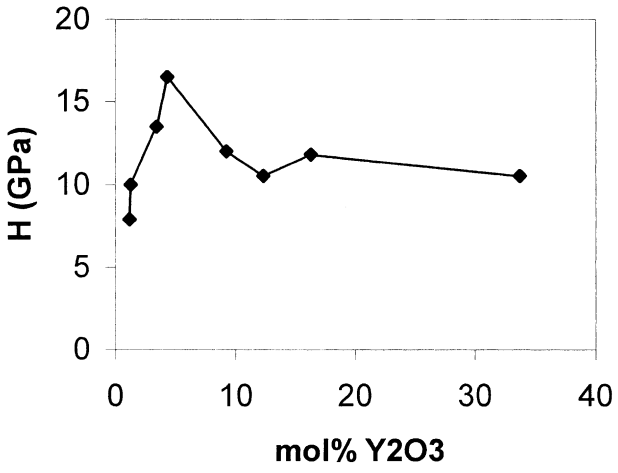

Fig. 2. Microhardness at room temperature of YSZ versus yttria content. Data from Hartmanova et al.[26]

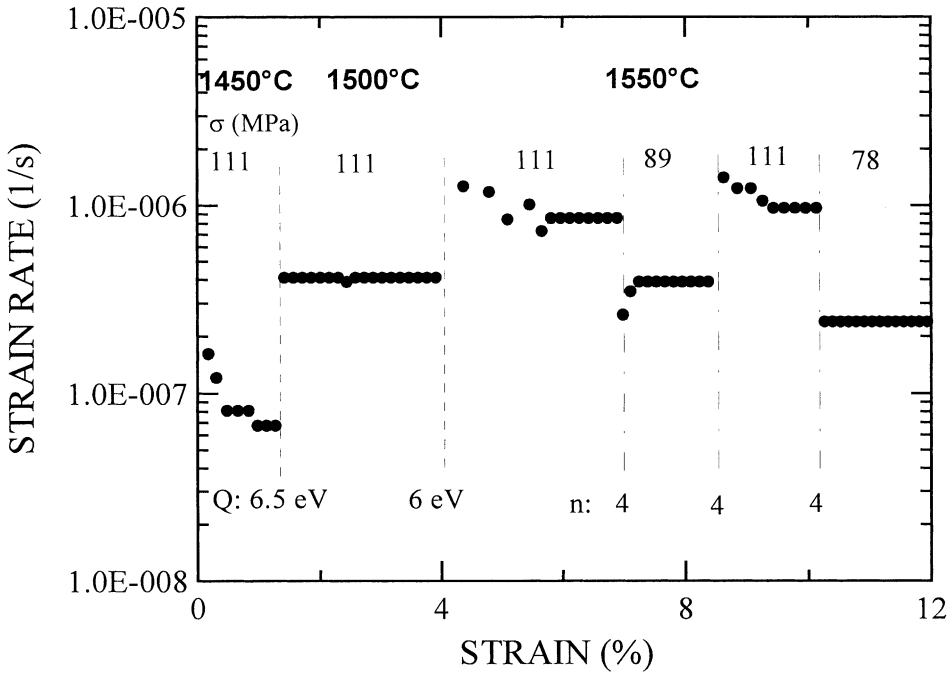

Fig. 3. Typical creep curve, strain rate versus strain, of a 32 mol% sample crept in Ar at 1400, 1450 and 1500 °C. The values of activation energy, Q, and stress exponent, n, have been estimated from the strain rate values at changes of temperature and load, respectively, as indicated in the text.

$$\dot{\varepsilon} = A\sigma^n \exp\left(\frac{-Q}{kT}\right) \quad (1)$$

The stress exponent, n and the activation energy, Q, yield information about the microscopic deformation mechanisms. They have been estimated using the procedure developed in Ref. 12. Once the creep test was finished, the samples were cooled down at 800 °C/h under reduced load (2–5 MPa).

The microstructure of undeformed and deformed samples has been studied via transmission electron microscopy (TEM). Foils were cut parallel to different crystallographic planes, such as the primary slip plane (001) and the climb plane $\left(1\bar{1}0\right)$, etc., and thinned to electron transparency by mechanical polishing followed by ion milling. Thin carbon films were evaporated on the samples to avoid electrical charging during observation. The microscopes used were a Hitachi H-800 (Servicio de Microscopía Electrónica de la Universidad de Sevilla), operating at 200 kV and a Phillips CM-300 (Los Alamos National Laboratory, USA) operating at 300 kV. Extinction studies ($\vec{g}\cdot\vec{b} = 0$) have been carried out to determine the Burgers vector of the dislocations and to identify the slip systems activated during deformation.

3. Results and discussion

3.1. Mechanical tests

Fig. 3 shows a typical creep plot of the strain rate versus strain. From the data obtained by temperature and stress changes during the tests, taking the extrapolation of the steady-state strain rate values and neglecting transients, values of n and Q were estimated in each experiment. These values did not vary significantly with the yttria content. Table 1 shows the average values for the stress exponent, n.

In order to compare the results from different experiments (different conditions of stress, σ, temperature, T, and strain rate, $\dot{\varepsilon}$), we have normalised the experimental values of strain rate to a stress of 100 MPa. Using Eq. (1) we can combine the expressions for an experimental

Table 1
Values of the stress exponent, n for 9.4 and 21 mol% YCSZ compared to the compositions studied in this work: 24, 28 and 32 mol%

Temperature range °C	Stress exponent (n)				
	9.4 mol%[7]	21 mol%[12]	24 mol%	28 mol%	32 mol%
$1400 < T < T_c$[a]	7.3±0.5	5.0±0.3	7.0±0.5	6.5±0.5	7.0±0.5
$1700 > T > T_c$[a]	4.5±0.4	3.2±0.4	4.5±0.5	4.9±0.5	4.8±0.5

[a] T_c, transition temperature, around 1500 °C.

$\dot{\varepsilon}_{exp}$ (known values of σ_{exp} and T) and a normalised $\dot{\varepsilon}_{100}$ (same T and $\sigma = 100$ MPa). The resulting expression is:

$$\dot{\varepsilon}_{100} = \dot{\varepsilon}_{exp}\left(\frac{100}{\sigma_{exp}}\right)^{n} \quad (2)$$

To estimate $\dot{\varepsilon}_{100}$ we have taken the experimental values of n from stress changes at each particular temperature. This procedure allows an evaluation of the influence of the yttria content. Fig. 4 displays the strain rate of 24, 28 and 32 mol% YCSZ extrapolated at 100 MPa versus $10^4/T$. With the y-axis in a log scale, the experimental points should adjust (through the least squares method) to a linear fit whose slope is related to the activation energy, Q, for the deformation mechanism: $Q = -m \cdot k \cdot 10^4$ eV, where m is the slope of the best fit and k is the Boltzmann constant. We can observe that all the compositions fit better to two linear fits with different slopes, which indicates the presence of two deformation mechanisms that take control at different temperatures. The two regimes of deformation, also reported for smaller yttria content,[7,9,12] can be observed with a transition temperature around 1500 °C. Table 2 shows the activation energies Q, measured from the slope of the Arrhenius plot in Fig. 4. The values of Q measured from individual temperature changes also agree with Table 2. The experimental values of n and Q have been compared to those measured in specimens of lower yttria content[7,9,12] in the same temperature interval.

The results shown in Tables 1 and 2 are in agreement with the previous ones for lower yttria contents. The different values for n and Q in the low and high-temperature ranges can be attributed to two different deformation mechanisms.

From Fig. 4 we observe that the strain rate for 24, 28 and 32 mol% is smaller (i.e. these materials are more creep resistant) than 21 mol% for the same experimental conditions. However, the differences within the range 24–32 mol% are not remarkable and fall into the experimental error margin. The scattering of the results comes from two contributions: the experimental error of the creep tests and the error due to the normalisation, (where a value for the stress exponent has to be assumed) which make it difficult to distinguish slight variations in the creep resistance. However, it is clear from the graph that there is a slight increase in the creep resistance between 21 mol% and higher yttria contents. We cannot establish a clear tendency within the 24, 28 and 32 mol%, but we can compare isolated values of the strain rate for the different yttria content at the same temperature and stress (to avoid normalisation). Individual values of strain-rate for a given temperature and stress are summarised in Table 3. Accordingly, a slight increase of the creep resistance has been found with increasing yttria content.

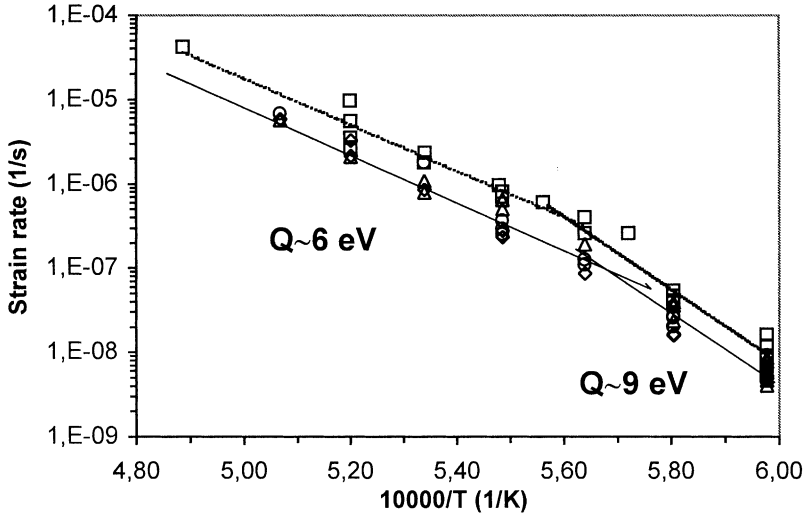

Fig. 4. Strain rate normalised at 100 MPa versus the inverse absolute temperature ($\dot{\varepsilon}_{100}$ versus $10^4/T$): (□) 21 mol%, (○) 24 mol%, (◇) 28 mol%, (△) 32 mol%.

Table 2
Values of activation energy, Q, for 9.4 and 21 mol% compared to the compositions studied in this work: 24, 28 and 32 mol% yttria YCSZ

Temperature range °C	Activation energy, Q (eV)				
	9.4 mol%[7]	21 mol%[12]	24 mol%	28 mol%	32 mol%
$1400 < T < T_c$[a]	7.5	9.0±0.5	9.0±0.5	9.6±0.5	9.0±0.5
$1700 > T > T_c$[a]	5.5	5.7±0.4	5.8±0.5	5.9±0.5	5.9±0.5

[a] T_c, transition temperature, around 1500 °C.

Table 3
Original experimental data from mechanical tests: strain rate at a given temperature and stress, and experimental values of stress exponent from individual load changes used for the normalisation of Fig. 4

T (°C)	σ (MPa)	$\dot{\varepsilon}$ (s^{-1})	n
21 mol%			
1500	104	3,60E-07	5
1550	104	9,30E-07	3
1600	104	2,0E-06	3
24 mol%			
1450	125	8,2E-08	5
1450	147	1,8E-07	5
1450	125	1,3E-07	5
1450	170	2,9E-07	5
1450	147	1,4E-07	5
1500	147	4,0E-07	4
1500	125	2,1E-07	3
1550	125	5,7E-07	3
1550	102	2,7E-07	3
1550	147	1,2E-06	3
1650	47	1,00E-06	3
1600	47	4,00E-07	2
1650	47	2,5E-06	3
1400	162	2,70E-07	7
1400	162	1,87E-07	7
1400	189	5,0E-07	7
1400	176	2,6E-07	7
1450	176	1,8E-06	7
1475	176	5,4E-06	5
1700	71	3,41E-06	2
1400	143	7,40E-08	7
1400	167	2,07E-07	7
1400	179	2,7E-07	7
1400	191	4,8E-07	7
28 mol%			
1400	179	5,00E-08	4
1450	179	3,00E-07	5
1450	208	6,40E-07	5
1450	268	2,20E-06	5
1450	149	4,90E-08	4
1500	149	1,90E-07	4
1550	149	3,00E-07	3
1550	179	7,50E-07	3
1550	208	2,50E-06	3
1450	143	8,00E-07	6
1475	143	2,00E-06	6
1650	107	3,70E-06	3
1600	107	8,80E-07	4
1600	134	5,6E-06	4
1600	120	2,8E-06	4
1600	94	7,0E-07	3
1650	94	1,9E-06	2
1700	94	5,1E-06	2
32 mol%			
1450	111	8,10E-08	6
1450	111	6,70E-08	6
1500	111	4,0E-07	6
1550	111	8,5E-07	5
1550	89	4,0E-07	4
1550	111	9,7E-07	4
1550	78	2,4E-07	4
1650	67	2,20E-06	4
1650	67	1,40E-06	4
1600	67	3,9E-07	4
1600	67	3,2E-07	4
1600	67	2,4E-07	4
1600	89	6,8E-07	4
1600	111	1,2E-06	4
1650	111	3,2E-06	4
1700	111	8,6E-06	4
1600	67	1,2E-07	4
1400	131	7,40E-08	6
1400	175	5,40E-07	8
1400	156	2,70E-07	7
1400	156	1,80E-07	7
1400	179	4,9E-07	8
1400	179	4,3E-07	8
1400	168	2,6E-07	7
1700	85	9,60E-06	3
1450	150	2,70E-07	6
1425	135	9,30E-08	6

Previous results for 1400 °C < T < 1450 °C, have been explained by glide controlled dislocation motion (solute drag mechanism) while for 1450° < T < 1700 °C, the existing models propose a climb controlled one. Activation energies reported for diffusion controlled deformation are between Q = 5.3–6.0 eV for 9.4 and 21 mol%.[7,9,12,29] These values agree quite well with our results at high temperature. The higher values of n and Q in the low-temperature range have been related to a solute drag deformation mechanism, where dislocation glide is limited by point defects forming "Cottrell clouds" around the dislocation cores. The increase of creep resistance with yttria content in this range is almost negligible, which can be explained because the high concentrations of substitutional atoms (correlated to the high yttria content) can saturate the dislocation cores. A climb controlled recovery creep mechanism is proposed in the high temperature range, where dislocation kinetics reaches a steady state in the process of dislocation creation and annihilation. The annihilation process would take place via dislocation climb, by the Weertman mechanism,[30] which predicts a stress exponent of 4.5, in agreement with the estimated values (4.5, 4.9 and 4.8 for 24, 28 and 32 mol% respectively, see Table 1). Therefore, an increase of the creep resistance with increasing yttria content is expected since the diffusion coefficient decreases with increasing yttria content in that range of composition.[31,32]

3.2. Microstuctural analysis

The dislocation substructure was examined via TEM for samples deformed at different temperatures. This allowed us to compare the microstructure in the low and high temperature range.

Fig. 5 shows a TEM micrograph of a 32 mol% sample deformed at 1700 °C cut parallel to the primary (001) slip plane. The dislocation density has been estimated as $\rho \approx 6 \cdot 10^{12}$ m^{-2}. The dislocation lines are mostly straight. Fig. 6 shows the dislocation substructure of a 24 mol% YCSZ sample crept at 1700 °C in two different zone axes, corresponding to a secondary {111} plane and a {121} plane, with different **g** vectors. They can be compared to Fig. 5, since both of them show a homogeneous dislocation network with different Burgers vectors, and several nodes. These dislocation networks are characteristic of high-temperature recovery controlled deformation. Features as the density of dislocations and the length and shape of dislocation lines are similar to those reported for samples of lower yttria contents in the same temperature range.[7,12] The microstructural observations support the conclusions drawn from the n and Q values obtained in the mechanical tests. Recovery creep seems to be the controlling mechanism for our materials deformed in the high-temperature range (1500–1700 °C).

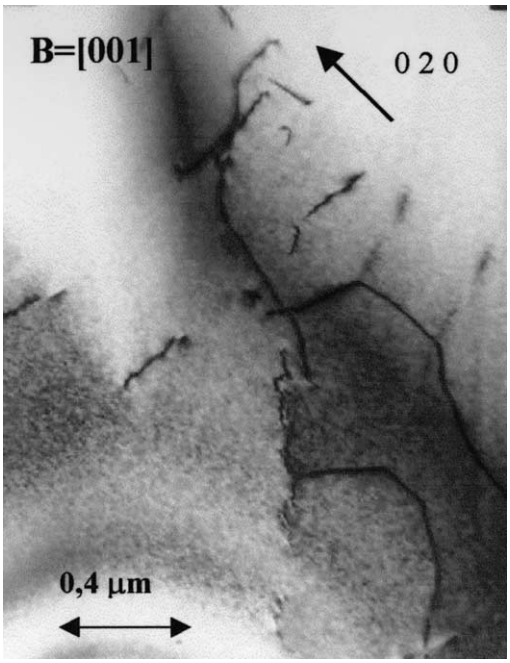

Fig. 5. TEM micrograph of 32 mol% YCSZ deformed at 1700 °C, parallel to the [001] primary slip plane.

Fig. 7 is a TEM micrograph of a 24 mol% YCSZ sample deformed at 1400° cut parallel to a {110} slip plane. The density of dislocations is much higher ($\rho \sim 5 \cdot 10^{13}$ m^{-2}) than at higher temperatures, and we can see an important quantity of curved dislocations and some dislocation loops. Only a few dislocations are found in non-slip planes. All these features are consistent with a mechanism based on glide like the solute drag mechanism, also reported for the same temperature and lower yttria contents.[7,12,33] Fig. 8 shows a foil of a 32 mol% YCSZ sample deformed at 1400 °C, cut parallel to a {110} plane. It shows a high dislocation density with some straight dislocations. This dislocation substructure is again typical of glide. The yttria content (in this range of compositions 24–32 mol%) does not affect the dislocation substructure after deformation. The solute drag model predicts the interaction of dislocations with Cottrell "clouds" of point defects,[34] in our case, substitutional yttrium atoms with different size than the zirconium ones.[35]

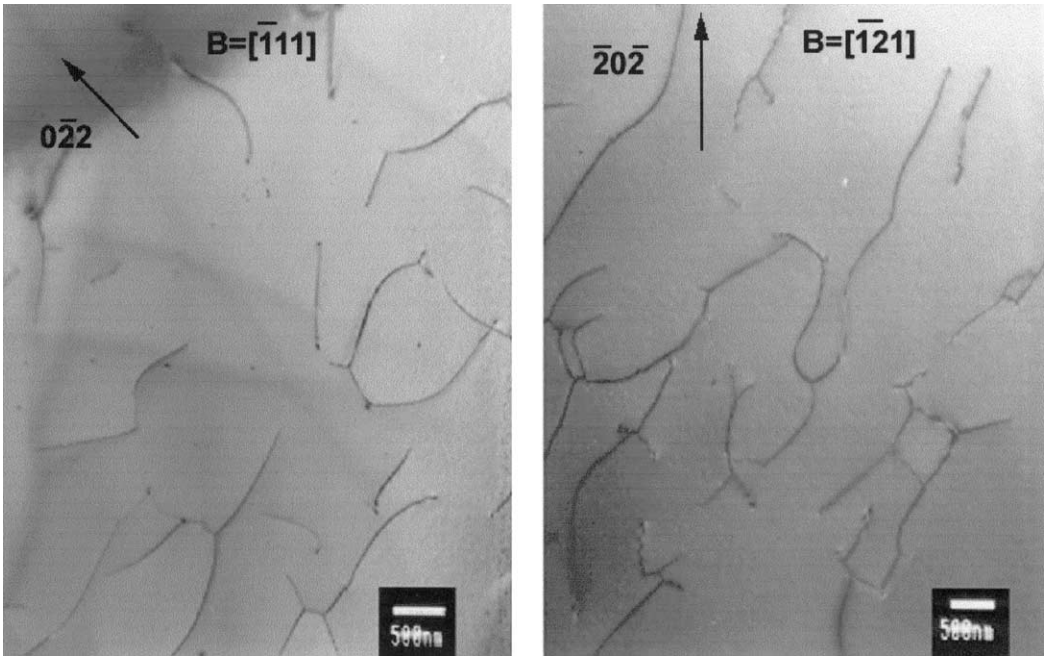

Fig. 6. TEM micrograph of a 24 mol% YCSZ sample crept at 1700 °C in two different zone axes, <111> and <121>, and with different **g** vectors.

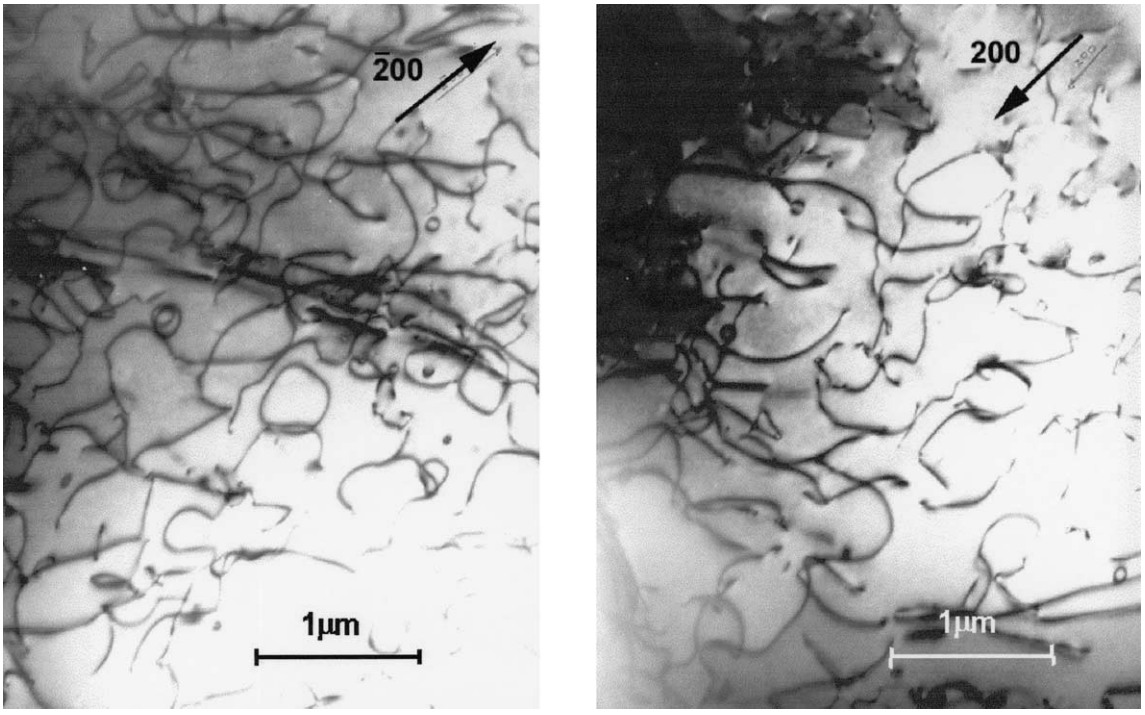

Fig. 7. TEM micrograph of a 32 mol% yttria YCSZ sample deformed at 1400 °C, parallel to a {110} plane, with two different **g** vectors.

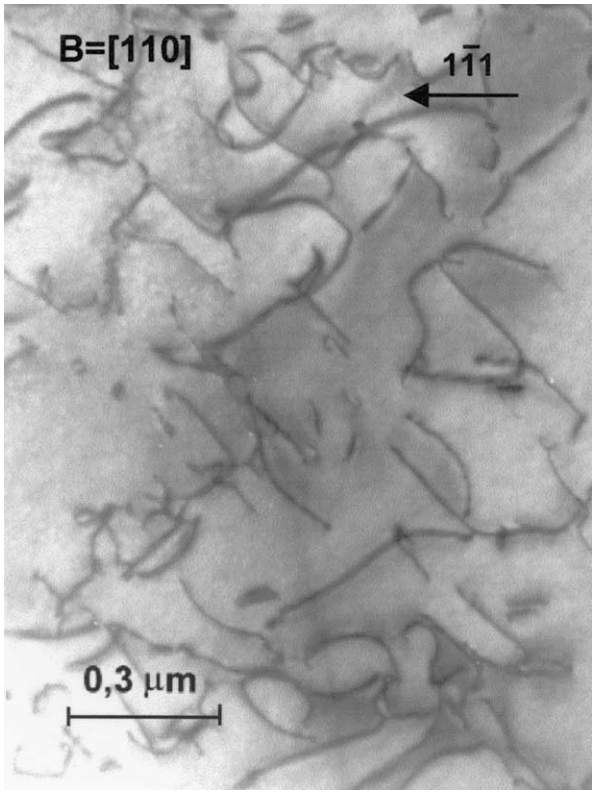

Fig. 8. TEM micrograph of a 32 mol% yttria YCSZ sample deformed at 1400 °C, parallel to a {110} plane.

The microstructural analysis by conventional TEM of YCSZ samples with 24, 28 and 32 mol% yttria yielded analogous results. This was expected, since the mechanical behaviour of the samples in this range of yttria content was not significantly different.

4. Conclusions

Different stress exponents and activation energies were obtained from the creep of 24, 28 and 32 mol% YCSZ samples depending on the temperature. The average values (for the three compositions) were: $n=6.8$ and $Q=9.2\pm0.5$ eV for 1400–1450 °C and $n=4.7$ and $Q=5.9\pm0.5$ eV for 1450–1700 °C. Therefore, two regimes of deformation can be distinguished, with a transition temperature around 1500 °C.

Samples deformed at 1400 °C show a higher density of dislocations on slip planes, with a significant percentage of curved dislocation lines and some dislocation loops. In the high-temperature range, however, the microstructure is different. The dislocation substructure of samples with different yttria content is analogous.

In view of the macroscopic parameters and microstructural observations, two mechanisms are proposed: glide controlled solute drag at the lower temperature (~1400 °C) and climb controlled recovery creep in the high-temperature range (1500–1700 °C).

The creep resistance reaches a plateau for yttria compositions ≥ 24 mol% in the low-temperature range, probably because the high concentration of point defects (substitutional yttrium atoms) saturates the dislocation cores. In the high-temperature range, the detected decrease of strain rate can be correlated to the very slight decrease of the cationic diffusion coefficient for YCSZ with increasing yttria content in the range of compositions under study.

Acknowledgements

The authors are very grateful to Dr. T.E. Mitchell and Dr. K.J. McClellan (LANL), as well as to other LANL researchers, for their valuable help during the experimental work, and for their time spent in useful discussions. One of the authors (A.G.-L.) wishes to thank Dr. U. Messerschmidt group for their kind welcome during a short visit to the MPI in Halle. Also thanks to Dr. J. Castaing for his support and advice during the hard part of the work. This work has been financed by the CICYT through the project MAT/97-1007-CO2-01 (Ministerio de Educación, Cultura y Deporte, Spain), as well as the CICYT fund MAT2000-0622.

References

1. Green, D. J., Hanninck, R. H. J. and Swain, M. V., *Transformation Toughening of Ceramics*. CRC Press, FL, 1989.
2. Wakai, F., Sakaguchi, S. and Matsukno, Y., *Adv. Ceram. Mater*., 1986, **1**, 259–263.
3. Bravo-León, A., Jiménez-Melendo, M. and Domínguez-Rodríguez, A., Mechanical and microstructural aspects of the high temperature plastic deformation of yttria-stabilized zirconia polycrystals. *Acta Metall. Mater*., 1992, **40**, 2717–2726.
4. Domínguez-Rodríguez, A., Lagerlöf, K. P. D. and Heuer, A. H., Plastic deformation and solid solution hardening of Y_2O_3-stabilized ZrO_2. *J. Am. Ceram. Soc*., 1986, **69**, 281.
5. Domínguez Rodríguez, A. and Heuer, A. H., Plastic deformation of Y_2O_3-stabilized ZrO_2 (YSZ) single crystals. *Cryst. Lattice Defects Amorphous Matter*., 1987, **16**, 117–123.
6. Lanteri, V., Domínguez-Rodríguez, A. and Heuer, A. H., High temperature precipitation hardening of Y_2O_3-partially-stabilized ZrO_2 (Y-PSZ) single crystals. *Acta Metall*., 1989, **37**, 559–562.
7. Martínez-Fernández, J., Jiménez-Melendo, M., Domínguez-Rodríguez, A. and Heuer, A. H., High-temperature creep of yttria-stabilized zirconia single crystals. *J. Am. Ceram. Soc*., 1990, **73**(8), 2452–2456.
8. Martínez-Fernández, J., Jiménez-Melendo, M., Domínguez-Rodríguez, A. and Heuer, A. H. In *Proceedings of Euroceramics 3, Engineering Ceramics*, ed. G. DeWith, R. A. Terpstra and R. Metselaar. Elsevier Publ. Co., London, 1989, pp. 3318-3322.
9. Jiménez-Melendo, M., Martínez-Fernández, J., Domínguez-Rodríguez, A. and Castaing, J., Dislocation climb controlled deformation of Y_2O_3-doped cubic ZrO_2 single crystals. *J. Eur. Ceram. Soc*., 1993, **12**, 97–101.
10. Domínguez-Rodríguez, A., Castaing, J. and Heuer, A. H., Dislocations and the mechanical properties of stabilized ZrO_2. *Rad. Effects Def. Sol*., 1991, **119–121**, 759.
11. McClellan, K. J., Sayir, H., Heuer, A. H., Sayir, A., Haggeerty, J. S. and Sigalovsky, J., *Ceram. Eng. Sci. Proc*., 1993, **14**, 651.
12. Gómez-García, D., Martínez-Fernández, J., Domínguez-Rodríguez, A., Eveno, P. and Castaing, J., Deformation mechanisms for high-temperature creep of high yttria content stabilized zirconia single crystals. *Acta Metall. Mater*., 1996, **44**(3), 991-999.
13. Gómez-García, D., Martínez-Fernández, J., Domínguez-Rodríguez, A. and Castaing, J., Mechanisms of high-temperature creep of fully stabilized zirconia single crystals as a function of the yttria content. *J. Am. Ceram. Soc*., 1997, **80**(7), 1668–1672.
14. Gómez-García, D., Martínez-Fernández, J., Domínguez-Rodríguez, A. and Westmacott, K. H., Electron-beam-induced loop formation on dislocations in yttria-fully stabilized zirconia. *J. Am. Ceram. Soc*., 1996, **79**(2), 2733–2738.
15. Fries, E., Guiberteau, F., Domínguez-Rodríguez, A., Cheong, D. S. and Heuer, A. H., High temperature plastic deformation of Y_2O_3-stabilized ZrO_2 single crystals I: the origin of the yield drop and associated glide polygonization. *Phil. Mag. A*, 1989, **60**, 107–121.
16. Cheong, D. S., Domínguez Rodríguez, A. and Heuer, A. H., High-temperature plastic deformation of Y_2O_3-stabilized ZrO_2 single crystals, II. Electron microscopy studies of dislocation substructures. *Phil. Mag. A*, 1989, **60**, 123–138.
17. Cheong, D. S., Domínguez Rodríguez, A. and Heuer, A. H., High-temperature plastic deformation of Y_2O_3-stabilized ZrO_2 single crystals, III. *Phil. Mag. A*, 1991, **63**, 377–388.
18. Baufeld, B., Bartsch, M., Messerschmidt, U. and Baither, D., Plastic deformation of cubic zirconia at temperatures between °C and 700 °C. *Acta Metall. Mater*., 1995, **1150**, 43 1925.
19. Baufeld, B., Petukhov, B. V., Bartsch, M. and Messerschmidt, U., *Acta Mater*., 1998, **46**(9), 3077–3085.
20. Messerschmidt, U., Baufeld, B., McClellan, K. J. and Heuer, A. H., Stress relaxation and solid solution hardening of cubic ZrO_2 single crystals. *Acta Metall. Mater*., 1995, **43**, 1917.
21. Baufeld, B., Baither, D., Bartsch, M. and Messerschmidt, U., Plastic deformation of cubic zirconia single crystals at °C. *Phys. Stat. Sol. (a)*, 1998, **1400**, 166 127-153.
22. Messerschmidt, U., Baufeld, B. and Baither, D., Plastic deformation of cubic zirconia single crystals. *Key Eng. Mater*., 1998, **153–154**, 143–182.
23. Messerschmidt, U., Baither, D., Baufeld, B. and Bartsch, M., Plastic deformation of zirconia single crystals: a review. *Mater. Sci. Eng*., 1997, **A233**, 61–74.
24. McClellan, K. J., *Structure/Property Relations in Y_2O_3-Stabilized Cubic ZrO_2 Single Crystals*. PhD thesis, Case Western Reserve University, Cleveland, OH, 1994.
25. Gallardo-López, A., Martínez-Fernández, J. and Domínguez-Rodríguez, A., Tensión de Límite Elástico en Monocristales de Circonia Totalmente Estabilizada con Alto Contenido en Óxido de Itrio. *Revista de Metalurgia*, 2000, **37**(II), 299–302.
26. Hartmanova, M., Schneider, J., Navratil, V., Kundracik, F., Schulz, H. and Lomonova, E. E., Correlation between microscopic and macroscopic properties of yttria stabilized zirconia—1. Single crystals. *Sol. State Ionics*, 2000, **136–137**, 107–113.
27. Domínguez Rodríguez, A., Cheong, D. S. and Heuer, A. H., High temperature plastic deformation in Y_2O_3-stabilized ZrO_2 single crystals: IV. The secondary slip systems. *Philos. Mag. A*, 1991, **64**, 923.
28. Gervais, H., Pellicier, B. and Castaing, J., Machine de Fluage pour Essais en Compression à Hautes Températures de Matériaux Céramiques, Rev. *Int. Hautes Temp. Refract*., 1978, **15**, 43.
29. Jiménez-Melendo, M., Domínguez-Rodríguez, A. and Bravo-León, A., *J. Am. Ceram. Soc*., 1998, **81**(11), 2761–2776.
30. Cahn, R. W. and Haansen, P., *Physical Metallurgy, Vol. II*. North Holland, Physics Publishing, Amsterdam, 1983 pp. 1326–1330..
31. Kilo, M., Borchardt, G., Weber, S., Scherrer, S. and Tinschert, K., Zirconium and calcium tracer diffusion in stabilized cubic zirconia. *Ber. Bunsenges. Phys. Chem*., 1997, **101**(9), 1361–1365.

32. Borchardt, G., Kilo, M., Weber, S., Scherrer, S., Lesage, B. and Kaitasov, O., Cation transport in yttria stabilized cubic zirconia: ^{96}Zr tracer diffusion in $(Zr_{1-x}\ Y_x)O_{2-x/2}$ single crystals with $0.16 \leqslant x \leqslant 0.64$. *Rad. Effects and Defects in Solids, 1998*.
33. Parthasarathy, T. A. and Hay, R. S., Effect of yttria concentration on low strain rate flow stress of cubic zirconia single crystals. *Acta Mater*., 1996, **44**(12), 4663–4676.
34. Friedel, *Dislocations*. Pergamon Press, 1964, pp. 368–384.
35. Gómez-García, D., Martínez-Fernández, J., Domínguez-Rodríguez, A. and Westmacott, K. H., *J. Am. Ceram. Soc*., 1996, **79**(2), 487–490.